Effects of Environmental Exposure to Iron Powder in Healthy and Elastase-Exposed Mice

Thiago Tafarel Galli
USP Medical School (FMUSP)
Elaine Cristina Campos
USP Medical School (FMUSP)
Leandro do Nascimento Camargo
Sírio-Libanês Hospital
Silvia Fukuzaki
Oswaldo Cruz German Hospital (HAOC)
Tabata Marayama dos Santos
USP Medical School (FMUSP)
Sara Sumie Sobral Hamaguchi
USP Medical School (FMUSP)
Suellen Karoline Moreira Bezerra
Fabio José Alencar Silva
USP Medical School (FMUSP)
Bianca Goulart Rezende
USP Medical School (FMUSP)
Fernanda Tenório Quirino dos Santos Lopes
USP Medical School (FMUSP)
Clarice Rosa Olivo
USP Medical School (FMUSP)
Beatriz Mangueira Saraiva-Romanholo
USP Medical School (FMUSP)
Carla Máximo Prado
Federal University of São Paulo (UNIFESP)
Edna Aparecida Leick
USP Medical School (FMUSP)
Christine L.M. Bourotte
USP Medical School (FMUSP)
Isabela Judith Martins Benseñor
USP Medical School (FMUSP)
Paulo Andrade Lotufo
USP Medical School (FMUSP)

Renato Fraga Righetti
USP Medical School (FMUSP)
Iolanda de Fátima Lopes Calvo Tibério (iocalvo@uol.com.br)
USP Medical School (FMUSP)

Article

Keywords:

Posted Date: July 25th, 2023

DOI: https://doi.org/10.21203/rs.3.rs-3090025/v1

Abstract

Background: Prolonged exposure to iron powder and other mineral dusts can harm affected populations, especially those with COPD. The goal of this study was to see how environmental exposure to metal dust affected lung mechanics, inflammation, remodeling, oxidative stress responses, and elastase in mice in two different mining centers in Vitória, ES, Brazil.

Methods: This study utilized 72 male C57Bl/6 mice (36 summer and 36 winter), which were divided into six groups: control, non-exposed (SAL); non-exposed, given elastase (ELA); exposed to metal powder at a mining company (SAL-L1 and ELA-L1); and exposed to a location three miles away from the mining company (SAL-L2 and ELA-L2) for four weeks. On the 29th day of the protocol, the researchers assessed lung mechanics, bronchoalveolar lavage fluid (BALF), inflammation, remodeling, oxidative stress, and alveolar wall alterations (mean linear intercept – Lm).

Results: ELA, ELA-L1 and ELA-L2 had an increase in Lm compared to the SAL groups ($p<0.05$). There was an increase in total cells and macrophages in ELA-L1 and ELA-L2 compared to the other groups ($p<0.05$). Exposed groups (ELA-L1, ELA-L2, SAL-L1, and SAL-L2) had an increase in cell expression of Inflammatory markers (IL-1β, IL-6, IL-10, IL-17, TNF-α, and neutrophils) ($p<0.05$); remodeling markers (TIMP-1, MMP-9, MMP-12, TGF-β, collagen fibers and MUC5AC); oxidative stress (iNOS); and mechanisms involved (NFkB) increased compared to ELA and SAL ($p<0.05$). Although we did not find differences in lung mechanics across all groups, there were low to moderate correlations between these parameters (elastance and resistance of lung tissue) (p0.05).

Conclusions: Aside from lung mechanics, environmental exposure to iron and metal powder exacerbated inflammation, remodeling, and oxidative stress responses in exposed mice with and without emphysema. The mechanisms involved are dependent on iNOS and NFkB activation.

INTRODUCTION

Environmental pollution is a major cause of disease, death, and disability in many countries worldwide. The World Health Organization (WHO) estimates that pollution causes approximately seven million deaths per year, in large cities and industrial centers around the world.[1] The increase in pollutant emissions has the potential to harm the health of exposed populations by causing, for example, irritations, allergies, respiratory and cancers.[2]

The city of Vitória is the major industrial center of the Brazilian state of Espírito Santo. The steel industry is the region's primary activity, and the majority of transportation is related to pellets, iron ore, coal, steel, and other products, resulting in increased emissions of particulate matter (PM) and ozone.[34]

Atmospheric particulate matter (APM) is a mixture of minute particles and liquid droplets ranging in size from coarse to fine to ultrafine. The composition of PM varies depending on where it is collected and may

contain remnants of fuel combustion such as polycyclic aromatic hydrocarbons (PAHs), sulfates, nitrates, microbes, and chemical elements such as iron, zinc, silicon, sodium, and aluminum.[5–7]

The harm caused by PM to the lungs increases as particle size decreases.[6] Small-sized particles remain suspended in the atmosphere for longer periods, increasing the likelihood of inhalation and posing a greater risk because they induce greater pulmonary resistance and inflammatory responses, increasing the risk of chronic lung inflammation and reduced lung functions.[8–11]

Chronic Obstructive Pulmonary Disease (COPD) is a heterogeneous pulmonary condition characterized to abnormalities of the airways and/or alveoli that remain persistent, often progressive, from airflow, caused by an inflammatory response to inhaled toxins.[12] It is now known that exposure to cigarette smoke, hazardous particles, or gases sets off an inflammatory chain reaction that produces a slew of potent cytokines and chemokines, resulting in chronic inflammation and tissue destruction in COPD patients However, the impact of exposure to iron ore processing on these individuals has yet to be determined.[13]

Because of industrialization and urbanization, the air quality in the city of Vitória's metropolitan region has deteriorated.[2] The particles in the region's air are made up of road dust (RD) resuspension, emissions from industrial activities, and marine aerosols. Samples of these particles contain high levels of aluminum and silicon, which are typical of soil composition. But they also contain higher levels of iron, chlorine, sodium, magnesium, and calcium than samples from other regions.[1]

Meteorological conditions have a significant impact on the dispersion or accumulation of pollutants.[12] Temperature, relative humidity, wind speed and direction, and other variables are all directly related to air pollution. Pollutant levels tend to rise when relative humidity and wind speed are low. Furthermore, the presence of rain and an increase in wind speed contribute to the dispersion and dilution of pollutants, resulting in a reduction in their concentration.[13]

Accordingly, the purpose of this study is to assess the effects of environmental exposure to iron dust and fine particles on healthy mice and elastase-exposed mice in two Brazilian cities (São Paulo and Vitória). In the city of Vitória, our research was carried out in two mining centers three miles apart, during two different seasons (summer and winter). Afterwards, we began to evaluate lung mechanics, inflammatory responses, extracellular matrix remodeling, and oxidative stress, as well as describe the mechanisms involved in this process.

MATERIALS AND METHODS

The present study was submitted and approved by the Review Board for Human and Animal Studies of the School of Medicine of the University of São Paulo (n° 919 – 17). Male C57Bl/6 mice (25–30 g, 7 weeks old, specific pathogen-free [SPF]) were obtained from the Animal Facility of the School of Medicine of the University of São Paulo. Animals were [14]maintained in controlled conditions of temperature (22 ± 2°C), humidity (70–75%), and dark/light cycle (12 h; lights on at 06:00 am) and allowed food and water

ad libitum. All animal care and experimental procedures followed the Guide for the Care and Use of Laboratory Animals also all animal experiments were conducted in accordance with ARRIVE guidelines.[14,15]

Animals

The study involved 72 mice, divided into two exposure periods (36 animals exposed in summer and 36 in winter). In each period, the animals were divided into six groups of six animals each: (1) SAL (6 animals): animals that received intratracheal instillation; (2) ELA (6 animals): animals that received intratracheal instillation of elastase; (3) SAL-L1 (6 animals): animals that received intratracheal instillation and were exposed to Place 1 in Vitória–ES; (4) ELA-L1 (6 animals): animals that received intratracheal instillation of elastase and were exposed to Place 1 in Vitória–ES; (5) SAL-L2 (6 animals): animals that received intratracheal instillation and were exposed to Place 2 in Vitória–ES; and (6) ELA-L2 (6 animals): animals that received intratracheal instillation of elastase and were exposed to Place 2 in Vitória–ES.

The animals from the SAL and ELA groups were kept in an animal care facility at the Medical School of the University of São Paulo. The temperature and humidity in the facility were controlled, and the racks where the animals stayed had pre-filters and high-efficiency particulate air filters that filtered particles greater than or equal to 0.3μm and removed microscopic contaminants from the air.

The groups of animals were sent to environmental exposure sites in the state in two different periods (summer and winter), they were exposed to a period of four weeks of continuous exposure to the environmental factors present in these specific locations, the animals were kept in rooms with controlled temperature, no sun exposure, light/dark cycle and food and water allowed *ad libitum*, but receiving outside air. During this period, they were carefully monitored to assess lung response and the effects of the environment on lung function and structure. Upon completion of the exposure period, the animals were carefully transported back to the city of São Paulo, in the state of São Paulo, Brazil.

Elastase-Induced Emphysema Model in Exposed Mice

C57Bl/6 mice were anesthetized with ketamine (40 mg/kg) and xylazine (5 mg/kg) via muscular injection. To spread the porcine pancreatic elastase (PPE) (0.667 IU mixed with 50 μL of sterile saline; elastase type I/E-1250, Sigma-Aldrich, St. Louis, MO, USA) throughout the lungs, the trachea was exposed and PPE was injected directly through it before chest compression (ELA, ELA-L1, and ELA-L2 groups). Using the same procedure, the control groups received 50 μL of sterile saline (SAL, SAL-L1, and SAL-L2 groups).[16]

After intratracheal instillation of elastase, the animals were exposed to both locations in the city of Vitória–ES. They remained there for four weeks before returning to the city of São Paulo–SP, Brazil, on the 29th day of the experimental protocol for pulmonary disease mechanics and pulmonary histopathology **(Fig. 1).**

Environmental Exposure

In the environmental exposure groups, the animals from both groups (SAL and ELA) were exposed to two locations in the city of Vitória, Espírito Santo state, Brazil **(**Fig. 2**).** In the region of the first location (“Place 1”), there are several mining companies whose primary activity is pelletizing iron ore powder, transforming it into spheres to facilitate sea transport, a process that generates iron-laden dust in the vicinity of the city's port and neighboring regions. Place 1 is located within one of the mining centers, where the pelletization of iron ore is carried out. On the other hand, the second location (“Place 2”) was the terrace of a hotel in Ilha do Boi, approximately three miles from Place 1. The local air current directs the pelletizing residues towards Place 2, resulting in the formation of PM and particle suspension.

These locations in the city of Vitória, Espírito Santo state, Brazil, were chosen because of the greater concentration of iron ore dust, as well as the shape of the bay at the Port of Tubarão, which favors the displacement of this material to the opposite location at Place 2, due to very strong wind currents in the region.

Due to climatic heterogeneity between seasons in Brazil, it was decided that the experiments would be carried out during two seasons with completely different climates, temperatures, humidity and wind speed and direction. Therefore, summer and winter were chosen. In the summer, there is an increase in rainfall, temperature and humidity. In the winter, temperatures are milder, precipitation is scarce and humidity levels are extremely low. Due to these climatic factors, it was necessary to send animals during two distinct seasons to evaluate and distinguish the climatic influence on particulate matter.

Evaluation of Pulmonary Mechanics

On day 29, animals were anesthetized (thiopental sodium, 33 mg/kg i.p.), tracheotomized, and placed in a plethysmograph chamber connected to a small animal ventilator (Harvard Apparatus, South Natick, MA, USA). To abolish their respiratory effort, the animals were given an intraperitoneal injection of pancuronium (0.2 mg/kg). Thereafter, data for oscillatory mechanics calculations was recorded. To this end, a signal that generated airflow oscillations with various raw frequencies (0.25 to 19.625 Hz) was used for 16 seconds, keeping the expiratory valve closed. The generated pressure values were then obtained and the airway impedance (Pressure/Flow) concerning the various frequencies produced was calculated. A 75% overlapping window was used in the 16-second signal and three blocks of eight seconds were used to calculate the oscillatory mechanics' parameters, according to the equation below:

$$Z(f) = Raw + i(2\pi f)Iaw + \frac{[Gtis - i*Htis]}{(2\pi f)^{\alpha}}$$

where Z(f) is the impedance of the respiratory system concerning frequency; Raw is the resistance of the airways; i is the imaginary unit (-1½); f is frequency; Iaw is airway inertance; and α = (2/π)* arctan (Htis/Gtis). And:

Ptr (t) = Ers x V (t) + Rrs x V '(t),

where Ptr is tracheal pressure; t is time; Ers is the elastance of the respiratory system; V is volume; Rrs is the resistance of the respiratory system; and V' is flow. In the ventilatory mechanics' calculations, the values respiratory system resistance (Rrs), respiratory system elastance (Ers), airway resistance (Raw), lung tissue resistance (Gtis), and lung tissue elastance (Htis) were expressed as a percentage increase from baseline.[16,17]

Bronchoalveolar Lavage Fluid Analysis

Following the evaluation of the respiratory system's mechanics, a bronchoalveolar lavage fluid (BALF) was performed. To begin, 1.5 mL of saline solution was injected into the tracheal cannula in three 0.5 mL doses. BALF was then centrifuged at 790 × g for 10 minutes at 5°C with an average recovery rate of 80%. The cell pellet was then rehydrated with 300 µL saline solution and vortexed. Subsequently, 100 µL was used to prepare a slide for differential cell counting. The remaining BALF was centrifuged onto a cytospin slide for six minutes at 450 rpm and stained with diff-quick.

Total cell counts were performed using light microscopy in a Neubauer hemocytometer (400×). The various cell types, such as neutrophils, eosinophils, lymphocytes, and macrophages, were identified using an optical microscope at 1,000x magnification. Each animal had approximately 200 cells counted.[18]

Lung Histology Analysis and Immunohistochemistry

We previously demonstrated that cytokine gene expression as measured by PCR yielded comparable results to morphometric analysis. Following immunohistochemistry studies, we chose to examine additional markers of inflammation, remodeling, and oxidative stress using only morphometric analysis.

Following the collection of BALF, the animals were bled and their hearts and lungs were extracted as a single unit. The lungs were then fixed in 4% formaldehyde at a constant pressure of 20 cmH2O for 24 hours before being stored in 70% alcohol for up to 36 hours before histological processing. Paraffin was used to embed pulmonary tissue fragments.

Five-micrometer slices of the lungs were prepared on sheets with (3-Aminopropyl) triethoxysilane (Sigma) and processed for histological analysis. The slices were deparaffinized, rehydrated, and treated with Proteinase K for 20 minutes at 37°C, followed by 20 minutes at room temperature, before being washed in phosphate-buffered saline (PBS). Endogenous peroxidase was blocked by incubating the slices for three 10-minute intervals in 3% hydrogen peroxide (H_2O_2).

The slices were stained with Picro-Sirius for collagen analysis and were also prepared for immunohistochemistry to evaluate markers such as MMP-9, MMP-12, TIMP-1, iNOS, NFkB, IL-6, IL-10, IL-17, IL-1β, TGF-β, TNF-α, MUC5AC, and neutrophil elastase. Each slice received a dilution of primary antibodies in Bovine Serum Albumin (BSA) solution. Table 1 describes the antibodies, their dilutions, and tags.

Table 1
– Marker, dilution, primary antibody and specifications.

Marker	Dilution	Primary Antibody	Specifications
IL-1β	1:200	Anti-rabbit	SC-7884; Sta Cruz Biotechnology, CA, USA
IL-6	1:100	Anti-rabbit	LS Bio Rabbit; Lifespan C746886
IL-10	1:150	Anti-goat	SC-1783 Goat monoclonal; Sta Cruz Biotechnology, CA, USA
IL-17	1:500	Anti-rabbit	SC-7927 Rabbit Polyclonal; Sta Cruz Biotechnology, CA, USA
Neutrophil Elastase	1:500	Anti-rabbit	Abcam Research, AB6872
TIMP-1	1:400	Anti-rabbit	LS-C299465 Mouse Polyclonal; Lifespan Bioscience, Inc., WA, USA
MMP-9	1:600	Anti-rabbit	SC-393859 Mouse Monoclonal; Sta Cruz Biotechnology, CA, USA
MMP-12	1:3000	Anti-rabbit	LS Bio Rabbit; Lifespan C295305
MUCAC	1:500	Anti-mouse	Abcam Research, AB3649
TGF-β	1:400	Anti-rabbit	SC-130348 Mouse Monoclonal; Sta Cruz Biotechnology, CA, USA
iNOS	1:500	Anti-rabbit	SC-7271 Rabbit Polyclonal; Sta Cruz Biotechnology, CA, USA
NFkB	1:500	Anti-rabbit	SC-8008 Mouse Monoclonal; Sta Cruz Biotechnology, CA, USA

The slices were then incubated overnight at 4°C in a cool, humid chamber. The slices were washed in PBS and incubated with secondary antibodies (as listed in Table 1) after 18 to 22 hours. After another PBS wash, the proteins were visualized with diaminobenzidine chromogen (DAB) (Sigma Chemical Co., St. Louis, MO, USA). Harris hematoxylin (Merck, Darmstadt, Germany) was used to counterstain the slices, and microscopy resin was used to mount them.[19]

Morphometric Analysis

Conventional morphometric analysis was performed using a 100-point, 50-line reticle attached to a microscope eyepiece. The total area of the reticle is 62,500 μm^2 at 400x magnification. The dot-counting technique was used to count the alveolar septa by superimposing the reticle onto the alveolar septum's peripheral regions. For each selected field, the ratio of positive cells to total points on the alveolar septa was calculated, and 10 fields per animal were evaluated at a magnification of 1,000x.[20,21]

Mean Linear Intercept (MLI) Measurement

A reticle consisting of 50 straight lines at 200x magnification was required for the microscopic analysis. For each slide, the alveolar septa in the outermost regions were examined in 15 different fields. The reticle was placed on top of the alveolar septa, and the intersections between the lines and the alveolar walls were counted. In this manner, the average diameter of the alveoli was calculated by taking into account the alveolar septum area and the number of intersections between the lines and the septum.[15] The Lm was then calculated using the following formula:

Lm = 2,500m / average number of intersections crossing the alveolar walls

Image Analysis

Collagen content was analyzed using an optical microscope and image analyzer. Images were captured by a DFC 420 camera, at 400x magnification, which was attached to a Leica DM2500 trinocular optical microscope (Leica Microsystems, Wetzlar, Germany), as well as analyzed using Image-Pro Plus 4.5 software (NIH, Bethesda, MD, USA). To detect fibers, the optical density measurement method was used, and the software informed of a threshold for positive areas and quantified them based on the determined area. Ten fields of alveolar septa per animal were examined. The results were expressed as a percentage of the positive area in comparison to the total area.[21,22]

Statistical Analysis

Scientific Graphing Software SigmaPlot® Version 11.0 was used for all statistical analyses. A one-way analysis of variance (ANOVA) followed by the Holm-Sidak method for multiple comparisons was used to assess differences between groups. These results were expressed as mean ± standard error. For correlation between variables, Pearson's correlation was used. For all analyses, $p < 0.05$ was considered statistically significant.

RESULTS

Lung Mechanics

In the evaluation of lung mechanics during the summer, there was a significant increase in %Rrs in SAL-L2 group compared to SAL group ($p \leq 0.05$). Similarly, there was an increase in %Rrs and %Raw in ELA group compared to SAL group ($p \leq 0.05$). However, there were no differences between groups in the analyses of %Ers, %Gtis and %Htis (Table 2).

Table 2

– Lung Mechanics and Positive Cell Values (± Standard Error): *p < 0.05 when compared to the SAL group; †p < 0.05 when compared to the ELA group; #p < 0.05 when compared to the SAL-L1 group; ††p < 0.05 when compared to the ELA-L1 group; &p < 0.05 when compared to the SAL-L2 group; and **p < 0.05 when compared to the ELA-L2 group.

SUMMER						
Lung Mechanics	SAL	SAL L1	SAL L2	ELA	ELA L1	ELA L2
Rrs ($cmH_2O.s.mL^{-1}$)	0.66 ± 0.02	0.80 ± 0.05	0.97 ± 0.08*	1.01 ± 0.10*	0.76 ± 0.04	0.80 ± 0.01
Ers ($cmH_2O.s.mL^{-1}$)	32.58 ± 1.49	35.86 ± 3.52	42.37 ± 2.15	39.73 ± 3.20	37.11 ± 3.65	38.59 ± 1.83
Raw ($cmH_2O.s.mL^{-1}$)	0.18 ± 0.02	0.28 ± 0.02	0.42 ± 0.09*	0.50 ± 0.12	0.28 ± 0.01	0.31 ± 0.03
Gits ($cmH2O.s^{(1-a)}.mL^{-1}$)	6.41 ± 0.53	6.80 ± 0.68	8.06 ± 0.29	6.05 ± 0.45	6.67 ± 0.56	6.94 ± 0.31
Hits ($cmH2O.s^{(1-a)}.mL^{-1}$)	33.30 ± 1.91	37.83 ± 3.53	40.71 ± 2.55	36.81 ± 4.79	42.95 ± 2.15	38.43 ± 1.87
Bronchoalveolar lavage Fluid (cells/10^4ml)						
Total cells	1.27 ± 0.11	0.79 ± 0.29	1.98 ± 0.50	3.43 ± 0.47*,#	2.20 ± 0.35	2.20 ± 0.48
Eosinophils	0.00 ± 0.00	0.00 ± 0.00	0.00 ± 0.00	0.01 ± 0.01	0.04 ± 0.01	0.16 ± 0.14
Neutrophils	0.00 ± 0.00	0.00 ± 0.00	0.15 ± 0.01	0.15 ± 0.15	0.11 ± 0.09	0.02 ± 0.01
Lymphocytes	0.00 ± 0.00	0.01 ± 0.01	0.01 ± 0.00	0.13 ± 0.07	0.02 ± 0.01	0.04 ± 0.01
Macrophages	1.13 ± 0.15	0.87 ± 0.27	1.91 ± 0.49	3.29 ± 0.42*,#	2.04 ± 0.30	2.14 ± 0.46
Inflammatory Markers (cells/$10^4\mu m^2$)						
IL-1β	1.79 ± 0.12	8.23 ± 0.55*,†	8.33 ± 0.53*,†	3.82 ± 0.37*	14.10 ± 0.73*,†,#,&	13.82 ± 0.77*,†,#,&
IL-6	4.38 ± 0.68	37.25 ± 0.93*,†	36.33 ± 0.87*,†	12.21 ± 0.63*	42.27 ± 0.71*,†,#,&	43.11 ± 0.66*,†,#,&
IL-10	7.25 ± 0.54	38.89 ± 0.80*,†	41.90 ± 0.30*,†	15.67 ± 1.18*	48.38 ± 0.42*,†,#,&	48.37 ± 0.84*,†,#,&

SUMMER						
IL- 17	6.52 ± 0.18	25.31 ± 1.93*,†	28.04 ± 1.38*,†	14.58 ± 1.69*	44.40 ± 1.65$^{*,\dagger,\#,\&}$	44.26 ± 1.48$^{*,\dagger,\#,\&}$
TNF - α	2.02 ± 0.22	44.39 ± 0.60*,†	44.82 ± 0.57*,†	4.91 ± 0.51*	50.55 ± 0.86$^{*,\dagger,\#,\&}$	50.72 ± 0.83$^{*,\dagger,\#,\&}$
Neutrophils	3.97 ± 0.40	9.67 ± 0.59*,†	9.97 ± 1.16*,†	6.63 ± 0.61*	13.11 ± 0.53$^{*,\dagger,\#,\&}$	12.63 ± 0.48$^{*,\dagger,\#,\&}$
Oxidative Stress (cells/10^4μm^2)						
iNOS	4.53 ± 0.62	32.54 ± 1.88*,†	32.81 ± 1.91*,†	13.56 ± 1.62*	53.08 ± 3.57$^{*,\dagger,\#,\&}$	53.21 ± 3.95$^{*,\dagger,\#,\&}$

As for the winter, there was a significant increase in %Raw in SAL-L2 group compared to SAL, as well as ELA-L1 and ELA-L2 groups ($p \leq 0.05$). But there were no differences between groups in the analyses of %Rrs, %Ers, %Gtis and %Htis (Table 3).

Table 3

– Lung Mechanics and Positive Cell Values (± Standard Error): *p < 0.05 when compared to the SAL group; †p < 0.05 when compared to the ELA group; $^{\#}$p < 0.05 when compared to the SAL-L1 group; ††p < 0.05 when compared to the ELA-L1 group, $^{\&}$p < 0.05 when compared to the SAL-L2 group; and **p < 0.05 when compared to the ELA-L2 group.

WINTER						
Lung Mechanics	SAL	SAL L1	SAL L2	ELA	ELA L1	ELA L2
Rrs ($cmH_2O.s.mL^{-1}$)	0.66 ± 0.02	0.77 ± 0.07	0.70 ± 0.10	0.83 ± 0.04	0.66 ± 0.05	0.61 ± 0.04
Ers ($cmH_2O.s.mL^{-1}$)	32.75 ± 2.32	41.69 ± 3.74	37.91 ± 5.63	34.22 ± 2.23	38.92 ± 4.04	32.29 ± 2.30
Raw ($cmH_2O.s.mL^{-1}$)	0.18 ± 0.01	0.23 ± 0.00	0.27 ± 0.030*,††,**	0.20 ± 0.02	0.17 ± 0.01	0.17 ± 0.01
Gits ($cmH2O.s^{(1-a)}.mL^{-1}$)	7.15 ± 0.25	7.42 ± 0.56	6.23 ± 0.51	5.92 ± 0.32	6.42 ± 0.53	6.27 ± 0.33
Hits ($cmH2O.s^{(1-a)}.mL^{-1}$)	28.91 ± 3.23	38.83 ± 2.84	36.88 ± 3.25	39.57 ± 3.36	43.91 ± 3.70	39.30 ± 3.10
Bronchoalveolar Lavage Fluid ($cells/10^4ml$)						
Total cells	2.68 ± 0.17	3.03 ± 0.89	2.95 ± 0.68	4.02 ± 0.51	8.10 ± 1.75$^{*,\dagger,\#,\&}$	8.82 ± 1.69$^{*,\dagger,\#,\&}$
Eosinophils	0.00 ± 0.00	0.09 ± 0.04*,†,††,**	0.04 ± 0.01	0.00 ± 0.00	0.00 ± 0.00	0.00 ± 0.00
Neutrophils	0.02 ± 0.01	0.17 ± 0.07*,†,††,**	0.08 ± 0.01	0.01 ± 0.00	0.00 ± 0.00	0.00 ± 0.00
Lymphocytes	0.00 ± 0.00	0.12 ± 0.04 *,††,**	0.04 ± 0.01	0.05 ± 0.02	0.00 ± 0.00	0.00 ± 0.00
Macrophages	2.65 ± 0.16	2.35 ± 0.76	2.78 ± 0.68	3.96 ± 0.50	8.12 ± 175$^{*,\dagger,\#,\&}$	8.83 ± 1.69$^{*,\dagger,\#,\&}$
Inflammatory Markers ($cells/10^4\mu m^2$)						
IL-1β	1.71 ± 0.17	8.52 ± 0.33*,†	8.84 ± 0.78*,†	4.02 ± 0.23*	13.68 ± 0.65 $^{*,\dagger,\#,\&}$	14.53 ± 0.69$^{*,\dagger,\#,\&}$
IL-6	4.16 ± 0.64	36.84 ± 1.21*,†	35.81 ± 1.11*,†	12.63 ± 0.73*	44.00 ± 1.51$^{*,\dagger,\#,\&}$	44.88 ± 1.96$^{*,\dagger,\#,\&}$

WINTER						
IL-10	6.91 ± 0.59	39.77 ± 1.17*,†	42.42 ± 0.97*,†	15.42 ± 1.15*	47.06 ± 0.79$^{*,\dagger,\#,\&}$	49.81 ± 1.11$^{*,\dagger,\#,\&}$
IL-17	7.22 ± 0.17	22.87 ± 0.58*,†	24.88 ± 1.26*,†	14.65 ± 0.12*	43.44 ± 2.55$^{*,\dagger,\#,\&}$	41.98 ± 0.57$^{*,\dagger,\#,\&}$
TNF-α	2.19 ± 0.27	44.47 ± 0.49*,†	44.09 ± 0.59*,†	4.29 ± 0.60*	50.20 ± 0.76$^{*,\dagger,\#,\&}$	51. 35 ± 0.61$^{*,\dagger,\#,\&}$
Neutrophils	3.85 ± 0.25	8.45 ± 0.33*	8.72 ± 1.05*	6.26 ± 0.54*	12.21 ± 0.72$^{*,\dagger,\#,\&}$	12.37 ± 1.03$^{*,\dagger,\#,\&}$
Oxidative Stress (cells/10^4μm^2)						
iNOS	5.21 ± 0.87	21.69 ± 2.08*	26.22 ± 1.71*,†	14.98 ± 1.33*	50.80 ± 3.92$^{*,\dagger,\#,\&}$	52.44 ± 2.93$^{*,\dagger,\#,\&}$

Bronchoalveolar Lavage Fluid Analysis

The number of total cells, eosinophils, neutrophils, lymphocytes, and macrophages in bronchoalveolar lavage in summer is shown in Table 2 and in winter in Table 3. In the summer, there were no differences in the number of total cells in bronchoalveolar lavage between SAL groups and ELA groups.

However, there was an increase in the number of total cells in ELA group compared to SAL and SAL-L1 groups ($p < 0.05$). The same pattern was observed in the analysis of macrophages, with no difference in the number of eosinophils, neutrophils, and lymphocytes between groups.

As for the winter, there was an increase in the number of total cells and macrophages in ELA-L1 and ELA-L2 groups compared to ELA group and SAL group ($p \leq 0.05$). Concerning the number of eosinophils, neutrophils, and lymphocytes, there was an increase in SAL-L1 group compared to SAL group, as well as compared to ELA-L1 and ELA-L2 groups ($p \leq 0.05$).

Mean Linear Intercept (Lm)

In both seasons, in the analysis of mean linear intercept (Lm), there were no differences between SAL groups and ELA groups. However, there was an increase in Lm in ELA, ELA-L1 and ELA-L2 groups compared to SAL, SAL-L1 and SAL-L2 groups, respectively ($p \leq 0.05$) **(**Fig. 3**).**

Inflammatory Markers

As for inflammatory markers in the summer (Table 2) and winter (Table 3), there was an increase in all inflammatory cytokines (IL-1β, IL-6, IL-10, IL-17, TNF-α, and neutrophils) in SAL-L1 and SAL-L2 groups compared to SAL group ($p \leq 0.05$), as well as in ELA-L1 and ELA-L2 groups compared to ELA group ($p \leq 0.05$). In the analysis between groups, there was an increase in inflammatory cytokines in ELA, SAL-L1, ELA-L1, SAL-L2 and ELA-L2 groups compared to SAL group ($p \leq 0 .05$).

In addition, there was also an increase in SAL-L1, ELA-L1, SAL-L2 and ELA-L2 groups compared to ELA group ($p \leq 0.05$), regarding all markers. Lastly, there was an increase in ELA-L1 and ELA-L2 groups compared to SAL-L1 and SAL-L2 groups ($p \leq 0.05$), regarding all markers.

Remodeling Markers

Remodeling markers during the summer (Fig. 4) (TIMP-1, MMP-9, MMP-12, TGF-β, collagen fibers and MUC5AC) increased in SAL-L1 and SAL-L2 groups compared to SAL group, as well as in ELA-L1 and ELA-L2 groups compared to ELA group ($p \leq 0.05$). When all groups were compared, there was an increase in SAL-L1, ELA-L1, SAL-L2 and ELA-L2 groups compared to SAL and ELA groups ($p \leq 0.05$), regarding all markers.

Collagen fibers, MMP-9, MMP-12, TGF-β, and MUC5AC also increased in ELA group compared to SAL group ($p \leq 0.05$). Furthermore, there was an increase in ELA-L1 and ELA-L2 groups compared to SAL-L1 and SAL-L2 groups ($p \leq 0.05$), regarding all markers. As for the winter, the results were similar to those of the summer (Fig. 5).

Oxidative Stress

iNOS

In the summer (Table 2), there was an increase in the number of positive cells for iNOS in SAL-L1 and SAL-L2 groups compared to SAL group ($p \leq 0.05$), as well as in ELA-L1 and ELA-L2 groups compared to ELA group ($p \leq 0.05$). When all groups were compared, there was an increase in ELA, SAL-L1, ELA-L1, SAL-L2, and ELA-L2 groups compared to SAL group ($p \leq 0 .05$), regarding all markers.

There was also an increase in SAL-L1, ELA-L1, SAL-L2, and ELA-L2 groups compared to ELA group ($p \leq 0.05$). Furthermore, there was an increase in ELA-L1 and ELA-L2 groups compared to SAL-L1 and SAL-L2 groups ($p \leq 0.05$), regarding all markers. As for the winter, the results were similar, with one exception: there was no difference in iNOS levels between SAL-L1 and ELA groups (Table 3).

Mechanisms Involved

NFkB

Both in the summer and winter (Fig. 6), there was an increase in the number of positive cells for NFkB in SAL-L1 and SAL-L2 groups compared to SAL group ($p < 0.05$). In ELA, ELA-L1, and ELA-L2 groups, there was also an increase in the number of cells compared to SAL group ($p < 0.05$), regarding all markers.

In addition, we observed an increase in NFkB in ELA-L1 and ELA-L2 groups compared to ELA group ($p < 0.05$), regarding all markers. The number of positive cells also increased in SAL-L1 and SAL-L2 groups compared to ELA group ($p < 0.05$), as well as in ELA-L1 and ELA-L2 groups compared to SAL-L1 and SAL-L2 groups ($p < 0.05$), regarding all markers.

Pearson's Correlation

In the summer, there were low to moderate correlations between lung tissue elastance and resistance (Gtis and Htis, respectively) and the following inflammatory markers: IL-1β (R = 0.465 p = 0.015, R = 0.447 p = 0.006), IL-6 (R = 0.465 p = 0.004, R = 0.386 p = 0.023), IL-10 (R = 0.484 p = 0.003, R = 0.435 p = 0.008), IL-17 (R = 0.434 p = 0.008, R = 0.349 p = 0.037), and TNF-α (R = 0.500 p = 0.002, R = 0.386 p = 0.020); as well as the following remodeling markers: TIMP-1 (R = 0.458 p = 0.005, R = 0.436 p = 0.008), MMP-9 (R = 0.476 p = 0.003, R = 0.416 p = 0.01), MMP-12 (R = 0.481 p = 0.003, R = 0.421 p = 0.01), and TGF-β (R = 0.496 p = 0.002, 0.387 p = 0.020). There was also a moderate correlation between collagen fibers and Gtis (0.472 p = 0.003); as well as the following oxidative stress markers: iNOS (R = 0.402 p = 0.015, R = 0.396 p = 0.017); and mechanism involved: NFkB (R = 0.477 p = 0.003, R = 0.411 p = 0.013).

In the winter, there was a correlation between Htis and the following inflammatory markers: IL-1β (R = 0.379 p = 0.023), IL-6 (R = 0.395 p = 0.017), IL-10 (R = 0.360 p = 0.031), IL-17 (R = 0.422 p = 0.010), TNF-α (R = 0.331 p = 0.049), and neutrophils (R = 0.496 p = 0.002); the following remodeling markers: TIMP-1 (R = 0.383 p = 0.021), MMP-9 (R = 0.433 p = 0.008), MMP-12 (R = 0.407 p = 0.014, 0.421 p = 0.01), TGF-β (0.394 p = 0.017), collagen fibers (R = 0.422 p = 0.010); as well as oxidative stress markers: iNOS (R = 0.435 p = 0.008); and mechanism involved: NFkB (R = 0.381 p = 0.021).

Qualitative Analysis

Representative photomicrographs (shown in Figs. 7 and 8 for the summer and winter, respectively) were taken to illustrate the inflammatory processes, mechanism involved, extracellular matrix remodeling and oxidative stress. The inflammatory processes are illustrated by IL-17; the mechanism involved by NFkB; the extracellular matrix remodeling characteristics by TIMP-1; and the oxidative stress markers by iNOS. All microphotographs were taken at 400x magnification.

DISCUSSION

This study demonstrates that environmental exposure in the city of Vitória, ES, promoted significant changes in inflammatory markers, oxidative stress, remodeling markers, and mechanisms involved (NFkB) of healthy animals. Such changes resulted in response patterns that are similar to those of the animals with elastase-induced emphysema, kept in a vivarium in São Paulo.

In this experimental model of emphysema, most analyses revealed that inflammatory markers, oxidative stress, remodeling markers, and mechanisms involved (NFkB) were higher in exposed groups compared to control animals kept in a vivarium in São Paulo. As a result, it is possible to conclude that local pollution promoted inflammation in healthy animals while exacerbating existing inflammation in animals with emphysema.

An increase in the number of people exposed to sulfur dioxide (SO_2) and nitrogen dioxide (NO_2) at World Health Organization-acceptable concentrations, as well as PM less than or equal to 10 μm in aerodynamic diameter (PM^{10}), has been linked to an increase in mortality caused by COPD exacerbation.[23]

In both seasons, there was no difference in lung mechanics between the groups. Nonetheless, there were low to moderate correlations between lung tissue elastance and resistance and indicators of inflammation, oxidative stress, and markers of remodeling and involved mechanisms. Hantos et al. (2008) discovered that mice given an intratracheal injection of elastase had an increase in volume and a decrease in lung tissue elastance but no change in airway and lung tissue resistance. This leads to the conclusion that lung tissue destruction is not always linked to lung system dysfunction.[24]

Mice exposed to fine particulate matter (PM) inhalation for four hours showed a slight but not significant increase in respiratory elastance and resistance.[25] There were no changes in lung function after two weeks of exposure to PM in a high-concentration environment; changes in lung function occurred only after four weeks of exposure.[26]

It should be noted that the animals in this study were exposed to ambient air in three different locations for four weeks, leading to the hypothesis that the exposure time was insufficient to cause changes in pulmonary mechanics.

Parallel to the experimental model analysis, Professor Christine Bourotte conducted a geochemical study of the region during the same summer and winter seasons to characterize the particulate material present. This revealed that the coarse fraction contained approximately 80% PM^{10}. For both collection sites and seasons, coarse PM concentrations were higher than fine PM concentrations.

Furthermore, in both summer and winter, mean concentrations at Place 1 were higher than at Place 2 (data not shown). PM enters the human body through breathing, and prolonged exposure to it can worsen lung inflammation due to its direct toxic effects and production of oxidative stress.[2]

It should also be noted that, in addition to the PM area, chemical composition is a key determinant of inflammatory response.[5] During Professor Christine Bourotte's analysis, the elements with the highest concentrations in the particulate matter were chlorine (Cl), iron (Fe), and sulfur (S). In the winter, chlorine concentrations were higher at Place 2 than at Place 1 in both coarse and fine materials (data not shown).

De Genaro et al. (2021) discovered that both acute and chronic exposure to chlorine gas reduces lung function and increases oxidative stress and mucus secretion in healthy mice.[26] When inhaled, chlorine can become solubilized in the bronchoalveolar fluid, cross the cell membrane, react with local proteins, activate local inflammation, and cause epithelial damage due to oxidative stress.[27–29]

When the pro-inflammatory signal is activated, reactive oxygen species (ROS) and pro-inflammatory cytokines such as TNF-α, IL-1β and interferon-gamma (INF-γ) are released, which activate induced nitric oxide synthase (iNOS).[30,31] At the site of inflammation, this enzyme produces nitric oxide (NO), which increases oxidative stress.[32] Pro-inflammatory cytokines can activate the Th17 response, resulting in the production of IL-17 and the recruitment of neutrophils, as well as tissue remodeling and mucus production.[33]

A single exposure to low doses of chlorine potentiated the Th2 response in asthmatic mice, resulting in increased inflammation, altered lung function, and activation of iNOS and kinase 2 (ROCK-2). Similar responses were observed in healthy animals exposed to low concentrations of chlorine.[34]

Recent research has revealed that several PM components can cause cellular harm, which in turn can activate pathways for extracellular matrix remodeling.[35,36] Airway remodeling refers to structural and extracellular matrix (ECM) changes in large and small airways.[37] According to research, the extracellular matrix (ECM) of the airway is altered in asthmatic patients, with a decrease in type IV collagen and elastin and an increase in type I collagen, fibronectin, laminin, periostin, versican, decorin, and lumican deposition.[37,38]

Pro-inflammatory factors such as cytokines and proteases are secreted, which further fuels immune responses and contributes to ECM remodeling.[39,40] Numerous immune cells, including but not limited to neutrophils, eosinophils, monocytes, macrophages, and mast cells, play a role in this.[39]

Even though PM^{10} is present in higher concentrations in the air of Vitória-ES, particles with diameters smaller than 2.5 μm can penetrate the bronchioles and alveoli, making it the most dangerous particle for the lungs.[34] Particles with this diameter distribution linger in the atmosphere for a longer period, increasing the likelihood of inhalation and the rate at which the composition of the air changes. The health consequences range from an increased risk of cardiovascular disease, chronic lung inflammation, and decreased lung function to an increase in asthma attacks.[10]

Chan et al. (2019) discovered an increase in lymphocytes and macrophages, which was also observed in exposure to high doses of PM. Nonetheless, exposure to 5 μg of PM^{10} did not result in the activation of

eosinophil or neutrophil-driven inflammation. As expected, the increase in IL-1β was linked to the activation of NLRP3 inflammasome.[42] In another study, daily exposure to 50 μg of $PM^{2.5}$ for three weeks increased both IL-1β and TGF-β1 levels in bronchoalveolar lavage fluid.[40]

According to Chu et al. (2016), $PM^{2.5}$ inhalation can exacerbate damage to macrophages in the air sacs of mice with COPD. They discovered that IL-6, IL-8, and TNF-α levels increased in bronchoalveolar lavage fluid, exacerbating airway inflammation. The researchers concluded that $PM^{2.5}$ can stimulate the expression of genes encoding TNF-α, IL-6, and IL-1β.[41]

When compared to the animals that remained in a vivarium, the animals exposed in Vitória showed a significant increase in all remodeling markers. Long-term chronic exposure to $PM^{2.5}$ resulted in impaired lung function, emphysematous lesions, airway inflammation, and airway wall remodeling. Exposure to $PM^{2.5}$ significantly increases the expression of MMP9, MMP12, fibronectin, collagen, and TGF-β1 proteins, regardless of concentration.[34]

Increased exposure to $PM^{2.5}$ can cause goblet cell hyperplasia and excessive mucus secretion in mice with COPD by increasing the expression levels of MUC5AC, MUC5B, collagen I, and collagen III in lung tissue.[26] MUC5AC increased in both exposure locations, both in SAL-L1 and SAL-L2 control groups, and in ELA-L1 and ELA-L2 elastase groups, with MUC5AC being higher in the ELA-L1 and ELA-L2 groups when compared to the other groups.

Wang et al. (2020) discovered that $PM^{2.5}$ has a significant impact on exacerbating COPD symptoms. According to the findings, $PM^{2.5}$ causes increased oxidative stress, airway inflammation, and goblet cell hyperplasia, which leads to imbalanced protease/antiprotease levels and airway remodeling. $PM^{2.5}$ deposited in the pulmonary bronchioles and alveoli causes oxidative stress, which sets off a chain reaction of harmful processes such as protease activation and increased bronchial inflammation, resulting in increased mucus hypersecretion, small airway fibrosis, and collagen buildup.[42]

As a result, there is persistent inflammation and the development of pulmonary emphysema.[42] Feng et al. (2019) discovered that mice exposed to high levels of $PM^{2.5}$ for four weeks had worsening lung function, mucus hypersecretion, and levels of pro-inflammatory cytokines and that oxidative stress indicators increased. According to the authors, four weeks may be sufficient time to achieve the histological changes caused by PM inhalation.[26]

When compared to the animals kept in a vivarium, those exposed in Vitória showed an increase in iNOS. The cytogenotoxic action of PM may be directly linked to oxidative stress. Several studies have been conducted to determine the cytogenotoxic action of PM,[46,47] which has been primarily attributed to metallic components bound or adsorbed on particles, particularly transition metals capable of inducing the formation of reactive oxygen species (ROS), such as iron.

Through the Haber-Weiss and Fenton reactions, iron particles stimulate the production of hydroxyl radicals, which causes oxidative stress in DNA, proteins, and lipids.[43,44] According to research, reactive oxygen species (ROS) can be produced on the surface of particles as a result of the absorption of polycyclic aromatic hydrocarbons (PAH) and nitro-PAH. The Fenton reaction, which is catalyzed by transition metals such as iron, copper, chromium, and vanadium, produces the highly reactive hydroxyl radical by combining Fe^{2+}, H_2O_2, and H^+, which can cause oxidative damage to DNA.[44]

Seaton et al. (2005) demonstrated that dust on the London Underground had cytotoxic and inflammatory potential at high doses, which was consistent with the dust's iron oxide composition.[45] The presence of soluble metals, such as iron, nickel, vanadium, cobalt, copper, and chromium, in inhaled particles may cause an increase in cellular oxidative stress in airway epithelial cells.[46]

Some free radicals generated from oxidative stress have been shown to activate specific protein transcription factors, including nuclear factor kappa B (NFkB), which increases the expression of genes for cytokines, chemokines, and other inflammatory mediators, as well as apoptosis and necrosis inducers of macrophages and respiratory epithelial cells, impairing organic defense and increasing airway reactivity.[47,48] In this study, NFkB levels were higher in SAL-L1, SAL-L2, ELA-L1, and ELA-L2 groups than in SAL and ELA groups, and in ELA-L1 and ELA-L2 groups than in SAL-L1 and SAL-L2 groups .

Unbalanced NFkB activation can result in excessive T cell activation, which is linked to autoimmune and inflammatory responses.[49] Activated CD4 + cells differentiate into various types of effector T cells (Th1, Th2, Th17, and follicular T cells) that produce cytokines and influence immune responses.[50] Inflammatory Th1 and Th17 cells are closely linked to IFN-γ secretion, which serves as cellular immunity defense and plays a role in inflammatory processes.[51] IL-17, a well-known inflammatory cytokine that attracts monocytes and neutrophils to the site of inflammation, is also released by Th17 cells.[52]

The use of an experimental animal model was a limitation of this study because it was not possible to directly extrapolate its findings to those expected in humans. Furthermore, the animals were stressed as a result of the environmental exposure being performed in another city, forcing the study's team to make two plane trips.

Despite this, the findings of this study emphasize the importance of investigating the effects of particulate matter exposure on lung tissue. This study aims to better understand these processes by examining inflammation, changes in the extracellular matrix, oxidative stress activation, and the signaling pathway responsible for these lung injury mechanisms.

Cellular expression of iNOS was deemed an appropriate marker in this study's evaluation of oxidative stress because elevated levels of these markers indicate inflammation development in healthy animals and exacerbation in animals with emphysema.

The goal of future research is to broaden the examination of oxidative stress by incorporating additional markers and delving deeper into anti-inflammatory cytokines. Furthermore, the presence of Th1, Th2, and Th17 cytokines was investigated, as well as a thorough examination of the remodeling process, which included an examination of collagen fibers, TIMP-1, MMP-9, MMP-12, TGF-β, and the NFkB signaling pathway.

CONCLUSIONS

With this study, it is possible to conclude that pollution exposure in the city of Vitória, ES, was responsible for the deterioration of pulmonary response in both emphysema and healthy animals. Furthermore, the mechanism involved in the activation of oxidative stress-related inflammatory markers appears to be linked to the expression of NFkB and a significant increase in iNOS.

References

1. WHO, 2020. Health Effects of Particulate Matter. Policy Implications for Countries in Eastern Europe, Caucasus and Central Asia. 2020. WHO Regional Office for Europe, Copenhagen.
2. Kyung, S. Y. & Jeong, S. H. Particulate-matter related respiratory diseases. Tuberc. Respir. Dis. (Seoul). 83, 116–121 (2020).
3. SANTOS, J.M.; REIS, N. C. *Caracterização e Quantificação de Partículas Sedimentadas na Região da Grande Vitória.* (2011).
4. Pedruzzi, R. *et al.* Performance evaluation of a photochemical model using different boundary conditions over the urban and industrialized metropolitan area of Vitória, Brazil. Env. Sci Pollut Res Int 26, 16125–16144 (2019).
5. Nani Guarieiro, L. L. & Nani Guarieiro, A. L. Vehicle Emissions: What Will Change with Use of Biofuel? in *Biofuels - Economy, Environment and Sustainability* (InTech, 2013). doi:10.5772/52513.
6. Xie, J., Teng, J., Fan, Y., Xie, R. & Shen, A. The short-term effects of air pollutants on hospitalizations for respiratory disease in Hefei, China. Int J Biometeorol 63, 315–326 (2019).
7. Yang, Y. *et al.* Continuous exposure of PM2.5 exacerbates ovalbumin-induced asthma in mouse lung via a JAK-STAT6 signaling pathway. Adv. Clin. Exp. Med. 29, 825–832 (2020).
8. de Haar, C., Hassing, I., Bol, M., Bleumink, R. & Pieters, R. Ultrafine but not fine particulate matter causes airway inflammation and allergic airway sensitization to co-administered antigen in mice. Clin Exp Allergy 36, 1469–1479 (2006).
9. Singh, S. *et al.* Endocytosis, oxidative stress and IL-8 expression in human lung epithelial cells upon treatment with fine and ultrafine TiO2: role of the specific surface area and of surface methylation of the particles. Toxicol Appl Pharmacol 222, 141–151 (2007).
10. Curtis, L., Rea, W., Smith-Willis, P., Fenyves, E. & Pan, Y. Adverse health effects of outdoor air pollutants. Env. Int 32, 815–830 (2006).

11. Zhao, Y. X. *et al.* Fine Particulate Matter-Induced Exacerbation of Allergic Asthma via Activation of T-cell Immunoglobulin and Mucin Domain 1. Chin Med J 131, 2461–2473 (2018).
12. GOLD. GLOBAL INITIATIVE FOR CHRONIC OBSTRUCTIVE LUNG DISEASE. Global strategy for Diagnosis, Management and Prevention of Chronic Obstructive Pulmonary Disease 2023 REPORT. Disponível em: <https://goldcopd.org/2023-gold-report-. (2023).
13. Baraldo, S. & Saetta, M. To reg or not to reg: that is the question in COPD. Eur Respir J 31, 486–488 (2008).
14. Percie du Sert, N. *et al.* The ARRIVE guidelines 2.0: Updated guidelines for reporting animal research. PLOS Biol. 18, e3000410 (2020).
15. National Research Council of The National Academies: Guide for the care and use of laboratory animals. 8th edn, (Natl Acad Press, 2011).
16. Martins-Olivera, B. T. *et al.* The Plant-Derived Bauhinia bauhinioides Kallikrein Proteinase Inhibitor (rBbKI) Attenuates Elastase-Induced Emphysema in Mice. *Mediat. Inflamm* 2016, 5346574 (2016).
17. Almeida-Reis, R. *et al.* Plant Proteinase Inhibitor BbCI Modulates Lung Inflammatory Responses and Mechanic and Remodeling Alterations Induced by Elastase in Mice. *Biomed Res Int* 2017, 8287125 (2017).
18. Saraiva-Romanholo, B. M. *et al.* Comparison of three methods for differential cell count in induced sputum. Chest 124, 1060–1066 (2003).
19. Possa, S. S. *et al.* Rho-kinase inhibition attenuates airway responsiveness, inflammation, matrix remodeling, and oxidative stress activation induced by chronic inflammation. Am J Physiol Lung Cell Mol Physiol 303, L939-52 (2012).
20. Leick-Maldonado, E. A. *et al.* Comparison of glucocorticoid and cysteinyl leukotriene receptor antagonist treatments in an experimental model of chronic airway inflammation in guinea-pigs. Clin Exp Allergy 34, 145–152 (2004).
21. Camargo, L. D. N. *et al.* Effects of Anti-IL-17 on Inflammation, Remodeling, and Oxidative Stress in an Experimental Model of Asthma Exacerbated by LPS. Front. Immunol. 8, (2018).
22. Righetti, R. F. *et al.* Effects of Rho-kinase inhibition in lung tissue with chronic inflammation. Respir Physiol Neurobiol 192, 134–146 (2014).
23. Franck, U., Odeh, S., Wiedensohler, A., Wehner, B. & Herbarth, O. The effect of particle size on cardiovascular disorders–the smaller the worse. Sci Total Env. 409, 4217–4221 (2011).
24. Hantos, Z. *et al.* Lung volumes and respiratory mechanics in elastase-induced emphysema in mice. J Appl Physiol 105, 1864–1872 (2008).
25. Amatullah, H. *et al.* Comparative cardiopulmonary effects of size-fractionated airborne particulate matter. Inhal Toxicol 24, 161–171 (2012).
26. Feng, S. *et al.* Hydrogen ameliorates lung injury in a rat model of subacute exposure to concentrated ambient PM2.5 via Aryl hydrocarbon receptor. Int Immunopharmacol 77, 105939 (2019).
27. Winder, C. The toxicology of chlorine. Environ. Res. 85, 105–114 (2001).

28. Hawkins, C. L., Pattison, D. I. & Davies, M. J. Hypochlorite-induced oxidation of amino acids, peptides and proteins. Amino Acids 25, 259–274 (2003).
29. Yadav, A. K. *et al.* Mechanisms and modification of chlorine-induced lung injury in animals. *Proc. Am. Thorac. Soc.* 7, 278–283 (2010).
30. Carlisle, M., Lam, A., Svendsen, E. R., Aggarwal, S. & Matalon, S. Chlorine-induced cardiopulmonary injury. Ann. N. Y. Acad. Sci. 1374, 159–167 (2016).
31. White, C. W. & Martin, J. G. Chlorine gas inhalation: Human clinical evidence of toxicity and experience in animal models. *Proc. Am. Thorac. Soc.* 7, 257–263 (2010).
32. Antosova, M. *et al.* Physiology of nitric oxide in the respiratory system. Physiol. Res. 66, S159–S172 (2017).
33. Aujla, S. J. & Alcorn, J. F. T H17 cells in asthma and inflammation. Biochim. Biophys. Acta - Gen. Subj. 1810, 1066–1079 (2011).
34. De Genaro, I. S. *et al.* Low dose of chlorine exposure exacerbates nasal and pulmonary allergic inflammation in mice. Int Immunopharmacol 77, 105939 (2018).
35. Li, W., Zhou, J., Chen, L., Luo, Z. & Zhao, Y. Lysyl oxidase, a critical intra- and extra-cellular target in the lung for cigarette smoke pathogenesis. Int. J. Environ. Res. Public Health 8, 161–184 (2011).
36. Zhou, G. *et al.* Hypoxia-induced alveolar epithelial-mesenchymal transition requires mitochondrial ROS and hypoxia-inducible factor 1. Am. J. Physiol. - Lung Cell. Mol. Physiol. 297, 1120–1130 (2009).
37. Hough, K. P. *et al.* Airway Remodeling in Asthma. Front. Med. 7, (2020).
38. Dekkers, B. G. J., Saad, S. I., van Spelde, L. J. & Burgess, J. K. Basement membranes in obstructive pulmonary diseases. Matrix Biol. Plus 12, 100092 (2021).
39. Helfrich, S., Mindt, B. C., Fritz, J. H. & Duerr, C. U. Group 2 innate lymphoid cells in respiratory allergic inflammation. Front. Immunol. 10, 1–12 (2019).
40. Zheng, R. *et al.* NLRP3 inflammasome activation and lung fibrosis caused by airborne fine particulate matter. Ecotoxicol. Environ. Saf. 163, 612–619 (2018).
41. Chu, X. *et al.* Effects of Astragalus and Codonopsis pilosula polysaccharides on alveolar macrophage phagocytosis and inflammation in chronic obstructive pulmonary disease mice exposed to PM2.5. Env. Toxicol Pharmacol 48, 76–84 (2016).
42. Wang, J. *et al.* Exposure to Air Pollution Exacerbates Inflammation in Rats with Preexisting COPD. *Mediat. Inflamm* 2020, 4260204 (2020).
43. Jung, M. H. *et al.* Genotoxic effects and oxidative stress induced by organic extracts of particulate matter(PM 10)collected from a subway tunnel in Seoul, Korea. Mutat Res 749, 39–47 (2012).
44. Lodovici, M. & Bigagli, E. Oxidative stress and air pollution exposure. *J Toxicol* 2011, 487074 (2011).
45. Seaton, A. *et al.* The London Underground: dust and hazards to health. Occup Env. Med 62, 355–362 (2005).

46. Zaremba, L. S. & Smoleński, W. H. Optimal portfolio choice under a liability constraint. Ann. Oper. Res. 97, 131–141 (2000).
47. Brook, R. D. *et al.* Air pollution and cardiovascular disease: a statement for healthcare professionals from the Expert Panel on Population and Prevention Science of the American Heart Association. Circulation 109, 2655–2671 (2004).
48. Rhoden, C. R., Lawrence, J., Godleski, J. J. & González-Flecha, B. N-acetylcysteine prevents lung inflammation after short-term inhalation exposure to concentrated ambient particles. Toxicol Sci 79, 296–303 (2004).
49. Chang, M. *et al.* The ubiquitin ligase Peli1 negatively regulates T cell activation and prevents autoimmunity. Nat Immunol 12, 1002–1009 (2011).
50. Zhu, J., Yamane, H. & Paul, W. E. Differentiation of effector CD4 + T cell populations. Annu. Rev. Immunol. 28, 445–489 (2010).
51. Oh, H. & Ghosh, S. NF-κB: roles and regulation in different CD4(+) T-cell subsets. Immunol Rev 252, 41–51 (2013).
52. Liu, C. W. *et al.* PM2.5-induced oxidative stress increases intercellular adhesion molecule-1 expression in lung epithelial cells through the IL-6/AKT/STAT3/NF-KB-dependent pathway. Part. Fibre Toxicol. 15, 1–16 (2018).

Figures

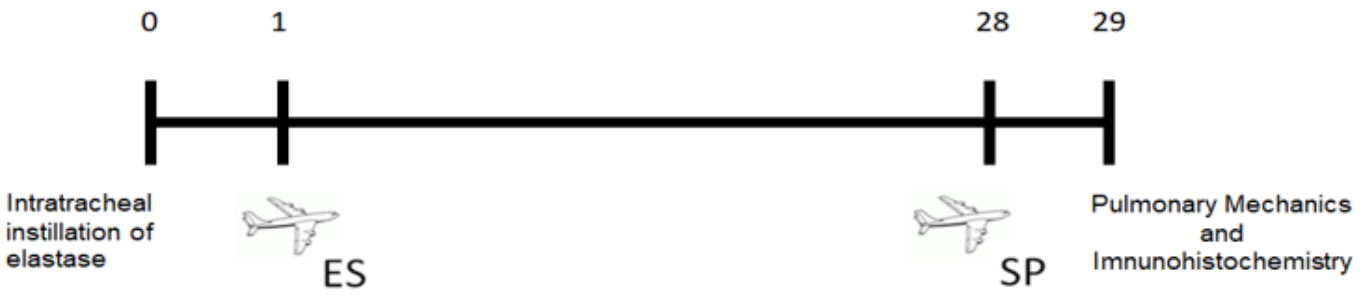

FIGURE 1 – Protocol for Elastase Induced Emphysema and Environmental Exposure

Figure 1

See image above for figure legend

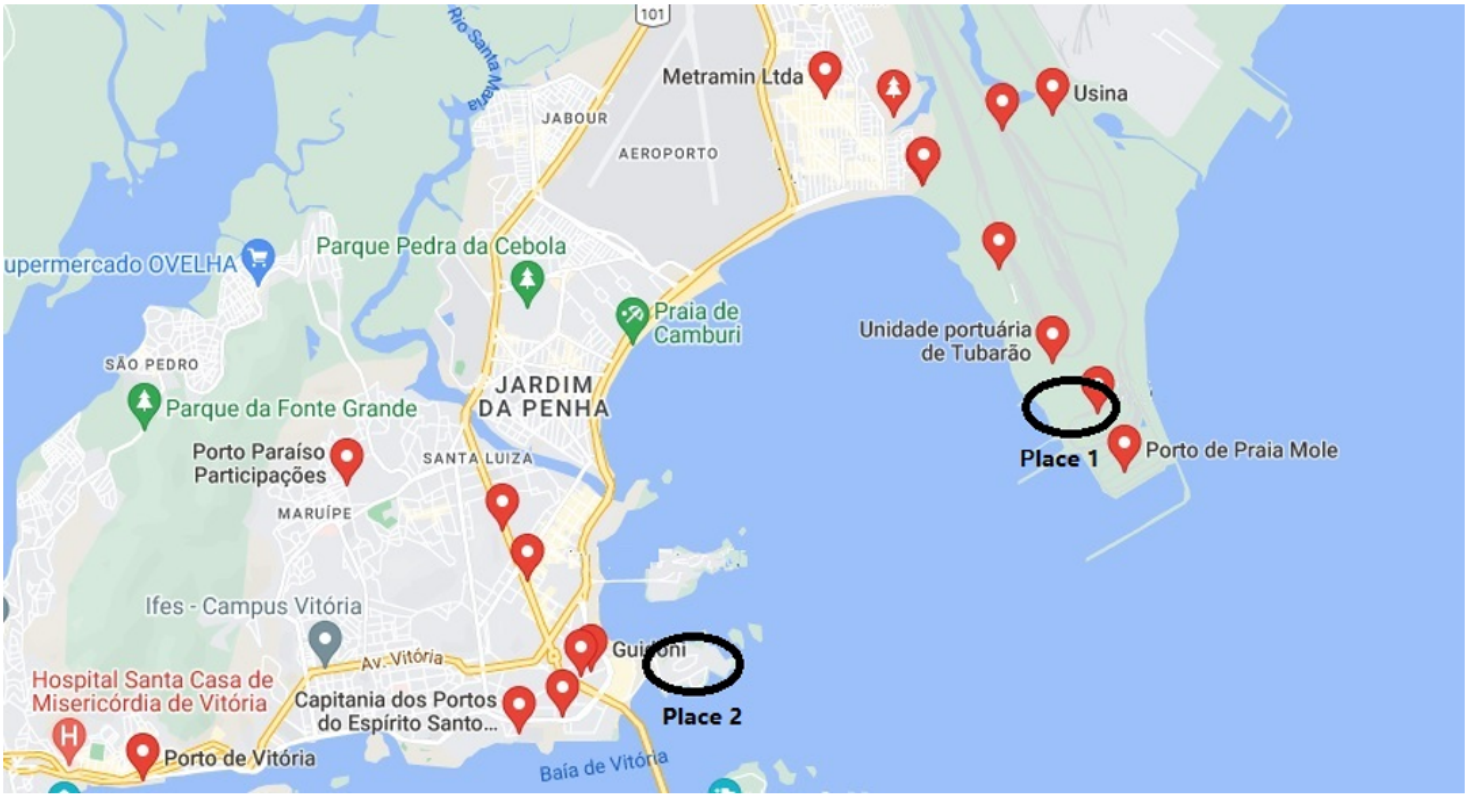

Figure 2

Locations of the mining centers in the city of Vitória, ES, Brazil. Source: Google Maps

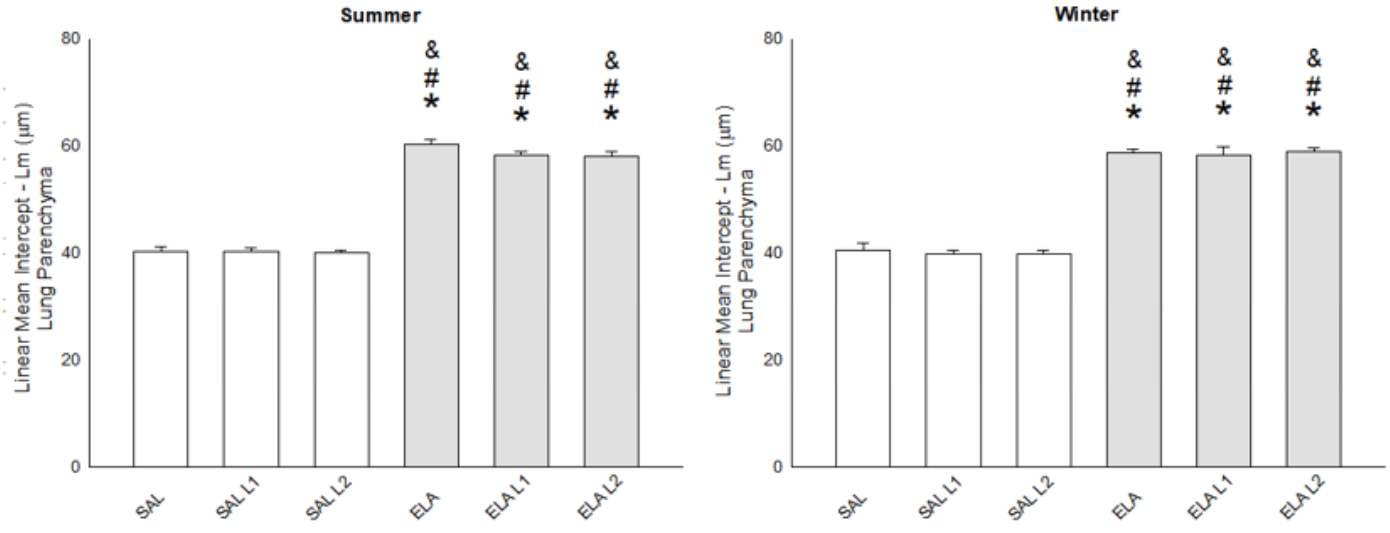

Figure 3

Mean Linear Intercept (µm^2 ± Standard Error): *p<0.05 when compared to the SAL group; $^{\#}$p<0.05 when compared to the SAL-L1 group; and $^{\&}$p<0.05 when compared to the SAL-L2 group.

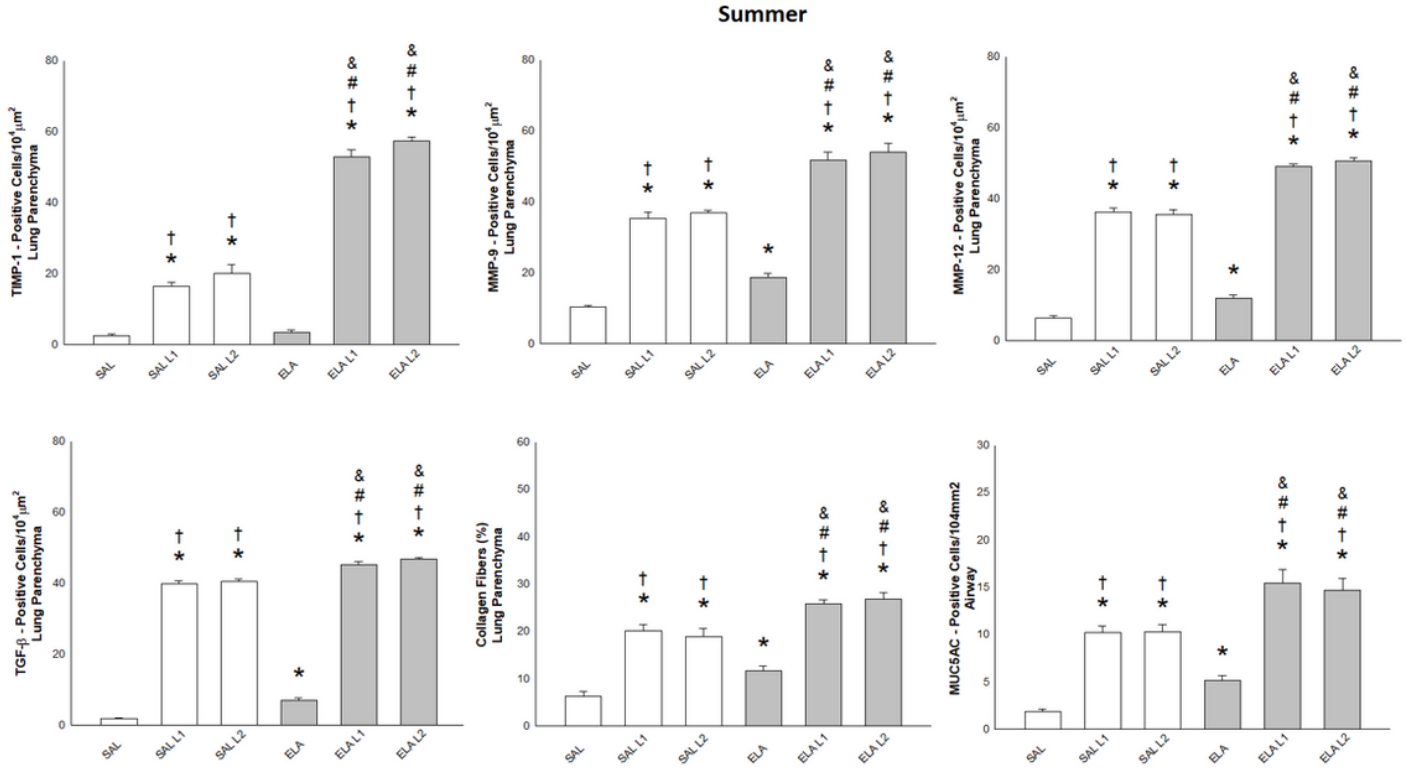

Figure 4

Remodeling Markers in Summer (TIMP-1, MMP-9, MMP-12, MUC5AC, and TGF-β) Positive Cell Values (Cells/10^4µm^2 ± Standard Error): *p<0.05 when compared to the SAL group; †p<0.05 when compared to the ELA group; $^{\#}$p<0.05 when compared to the SAL-L1 group; ††p<0.05 when compared to the ELA-L1 group, $^{\&}$p<0.05 when compared to the SAL-L2 group; and **p<0.05 when compared to the ELA-L2 group.

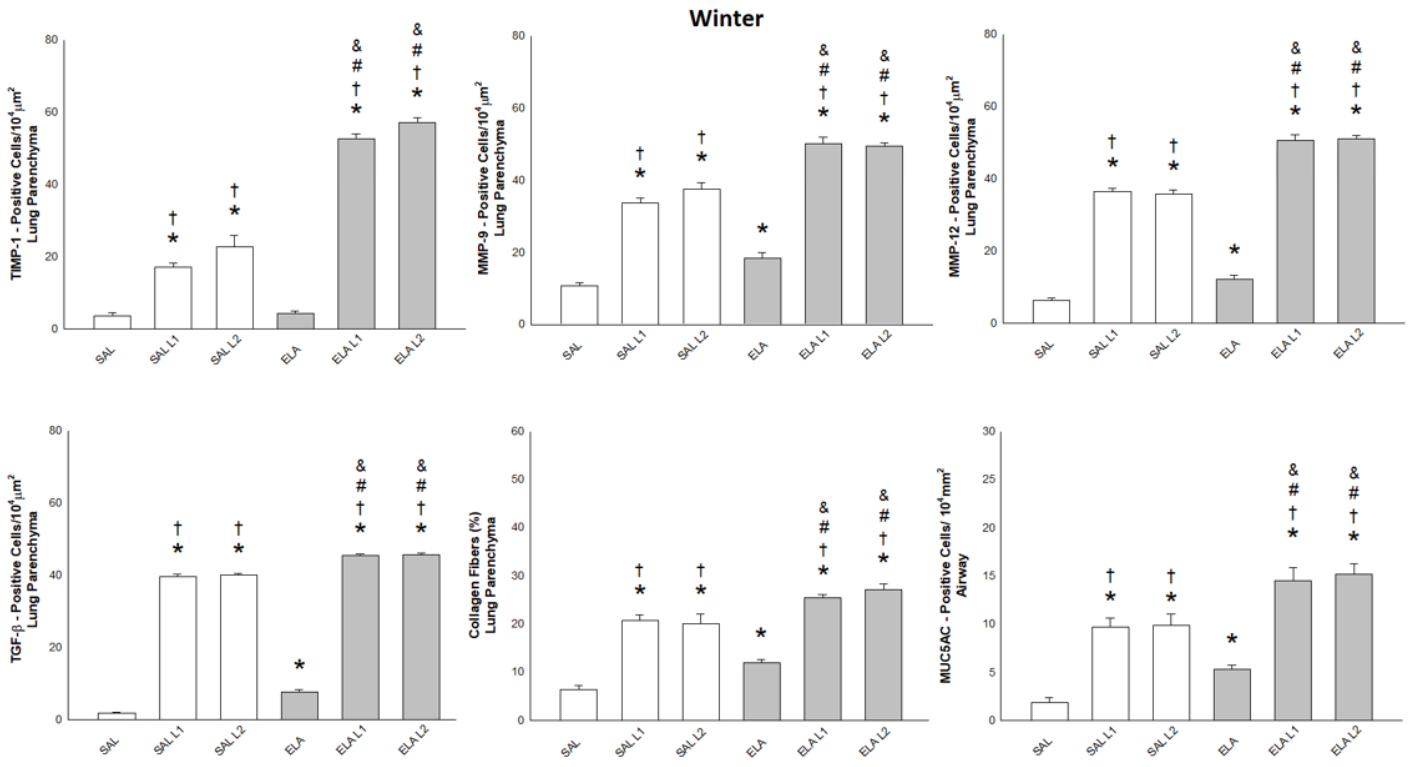

Figure 5

Remodeling Markers in Winter (TIMP-1, MMP-9, MMP-12, MUC5AC, and TGF-β) Positive Cell Values (Cells/$10^4\mu m^2$ ± Standard Error): *p<0.05 when compared to the SAL group; †p<0.05 when compared to the ELA group; $^{\#}$p<0.05 when compared to the SAL-L1 group; ††p<0.05 when compared to the ELA-L1 group, $^{\&}$p<0.05 when compared to the SAL-L2 group; and **p<0.05 when compared to the ELA-L2 group.

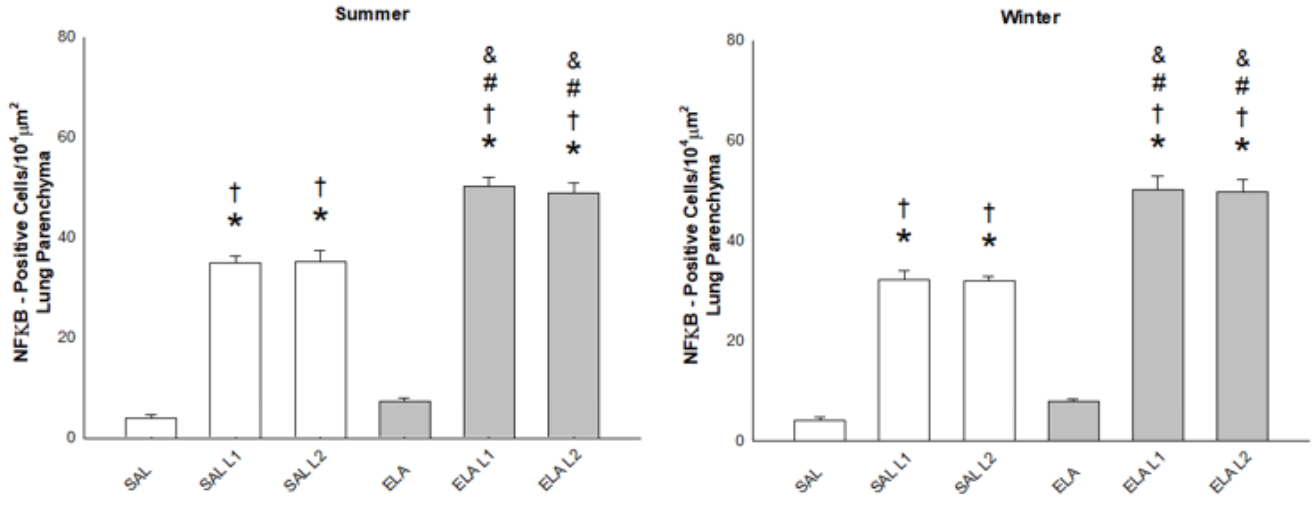

Figure 6

NFkB Positive Cell Values (Cells/10^4µm^2 ± Standard Error): *p<0.05 when compared to the SAL group; †p<0.05 when compared to the ELA group; $^{\#}$p<0.05 when compared to the SAL-L1 group; ††p<0.05 when compared to the ELA-L1 group, $^{\&}$p<0.05 when compared to the SAL-L2 group; and **p<0.05 when compared to the ELA-L2 group.

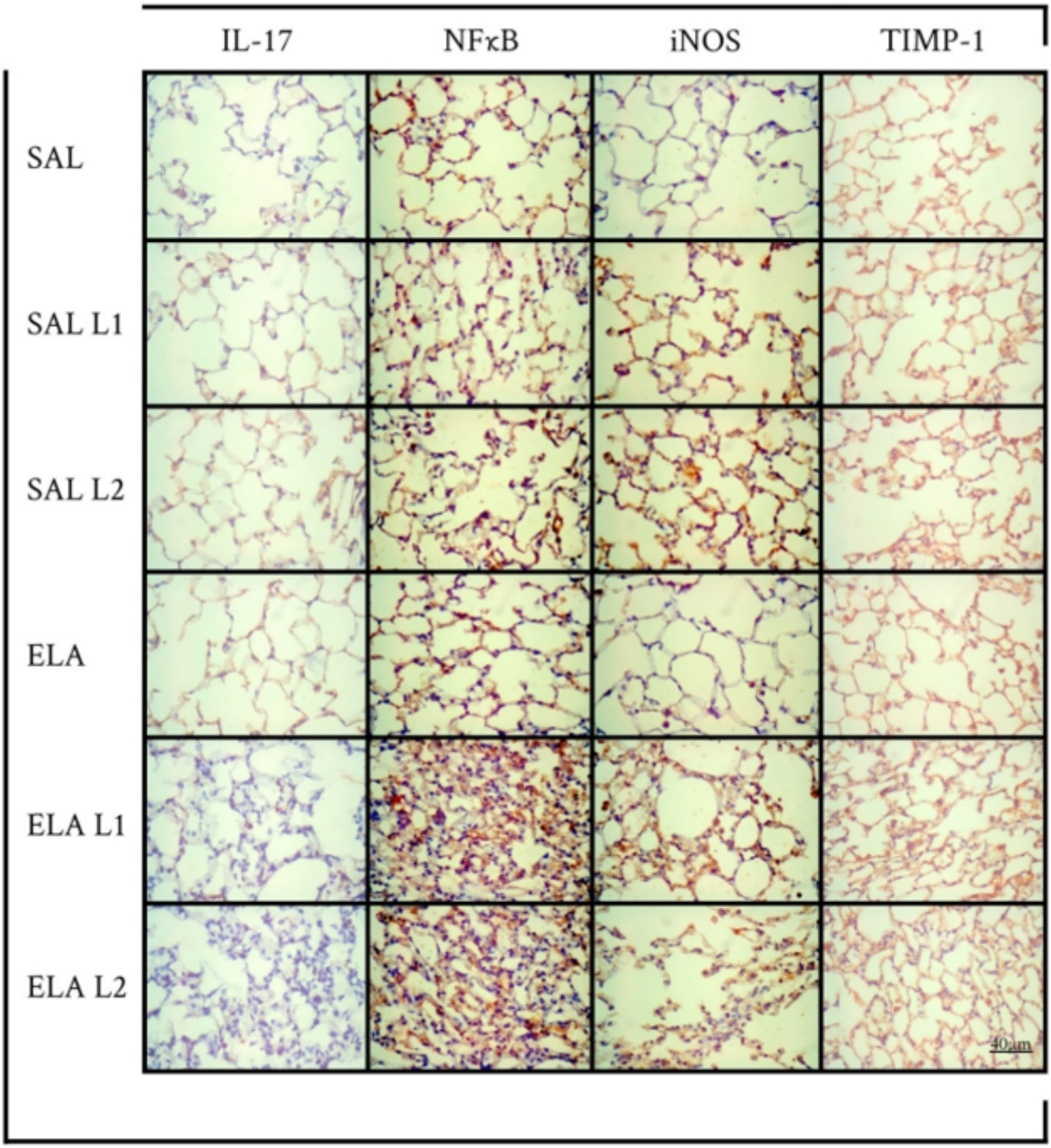

Figure 7

Inflammatory, Extracellular Matrix Remodeling, and Oxidative Stress Markers: Photomicrographs of IL-17, NFkB, iNOS, and TIMP-1. Immunohistochemical stain in the airways. 400× magnification. All experimental groups are represented: SAL, SAL-L1, SAL-L2, ELA, ELA-L1, and ELA-L2, in summer.

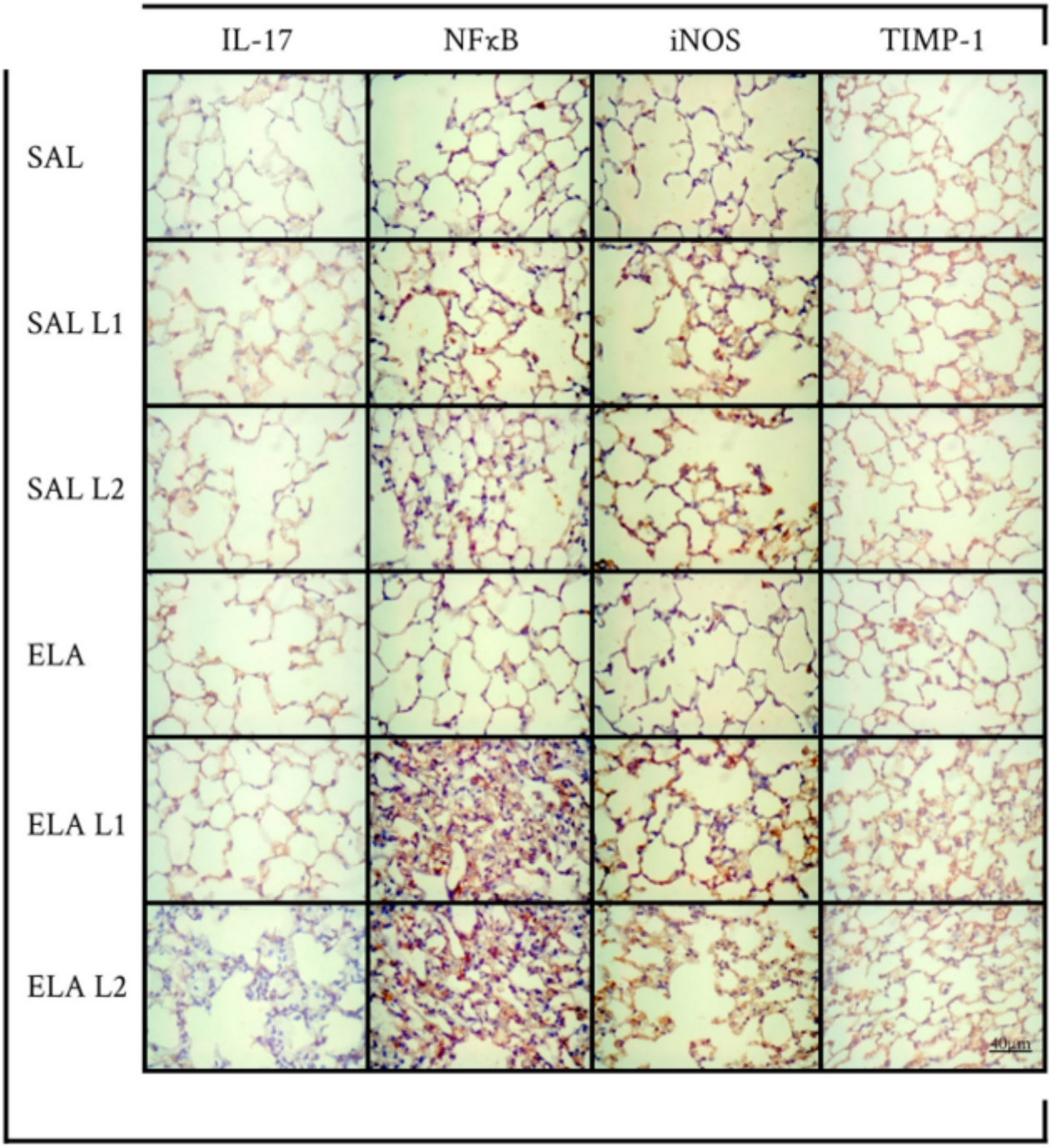

Figure 8

Inflammatory, Extracellular Matrix Remodeling, and Oxidative Stress Markers: Photomicrographs of IL-17, NFkB, iNOS, and TIMP-1. Immunohistochemical stain in the airways. 400× magnification. All experimental groups are represented: SAL, SAL-L1, SAL-L2, ELA, ELA-L1, and ELA-L2, in winter.